

Mixing and Transfer of Elements by Triaxiality

Daniel Friedli

*Département de Physique and Observatoire du Mont Mégantic,
Université Laval, Québec, Qc, G1K 7P4, Canada; dfriedli@phy.ulaval.ca*

Abstract. Various large-scale processes induced by triaxial potentials and able to alter stellar and gaseous abundance profiles are reviewed. In particular, strong bars can quickly and efficiently blend stars through chaotic mixing, and entail intricate inflows/outflows of gas. Bar-generated abundance features include flattenings, breaks, and plateaus in radial gradients as well as box- or peanut-like morphologies.

1. Introduction

In the world of galaxies, triaxial structures are very common. Fast-rotating ones include stellar bars which are present in at least two thirds of disk galaxies (Sellwood & Wilkinson 1993), whereas nearly 100% of Magellanic-type galaxies host bars (Odehahn 1996). Gaseous bars might also be present in primordial disks. Slow- or non-rotating triaxial potentials probably include bright ellipticals, but not faint ones (Merritt & Valluri 1996). Triaxial systems have at least two outstanding properties: they may contain irregular (chaotic) orbits, and they induce gravitational torques. These characteristics lead both to large-scale diffusion and mixing of stars, and produce transfer of angular momentum and matter; here, large-scale means $\gtrsim 1$ kpc. For mechanisms involved at smaller scales, see for instance Roy & Kunth (1995) and Elmegreen (this volume).

Stellar and gaseous components have distinct dynamics. The stellar one is mainly affected by large-scale mixing processes like *chaotic mixing*, which is generated by irregular orbits in triaxial potentials. Other mixing processes include the well-known *phase mixing* which operates e.g. through differential rotation, and *violent relaxation* which is relevant in strongly time-dependent potentials as present during galaxy formation and mergings (Binney & Tremaine 1987). Diffusion by encounters is also important but will not be discussed here (see e.g. Binney & Lacey 1988). On the contrary, the cold or warm gaseous components are essentially affected by transfer processes, which operate via *gravitational*, *viscous*, or *magnetic torques*. At kpc scales in strongly non-axisymmetric potentials, gravitational torques generally dominate over the two others.

Stellar abundances are becoming available for external galaxies, either from individual stars (Monteverde et al. 1997), or from integrated light (Beauchamp 1997). Numerical models presented in Sect. 2.2 thus provide predictions which still have to be confirmed by observations. On the contrary, numerous abundance determinations exist for the gas phase (Henry, this volume), and numerical results can be compared to observations (Sect. 3.2).

2. Mixing and Transfer of Stars

2.1. Chaos in Triaxial Systems

Barred Galaxies. Many investigations have been dedicated to the study of stellar orbits in barred potentials (e.g. reviews by Contopoulos & Grosbøl 1989; Sellwood & Wilkinson 1993). For these systems, one of the most remarkable discoveries is the possible existence of irregular orbits able to tour the whole phase space in less than a Hubble time τ_H . These chaotic orbits are present around the main resonances, especially the corotation resonance (CR). Their fraction increases when bar strength (Athanasoula et al. 1983), central mass concentration (Hasan & Norman 1990), noise or asymmetries (Habid et al. 1997) increase. In a recent study on the vertical orbital structure around CR, Ollé & Pfenniger (1998) have found that significant and fast radial and vertical diffusions take place when a critical bar strength is reached. The reason is that the Lagrangian points $L_{4,5}$ are then becoming “complex unstable”. The analysis of the population of self-consistent quasi-stable N-body strong bars, in 2D (Sparke & Sellwood 1987) or 3D (Pfenniger & Friedli 1991), has revealed that typically $\sim 35\%$ of orbits are chaotic (*hot population*), $\sim 45\%$ are confined inside the bar region (*bar population*), and $\sim 20\%$ are in the disk region (*disk population*). The high number of chaotic orbits clearly suggests that chaotic mixing should be important in such galaxies and might have dramatic consequences on stellar abundance profiles as will be discussed in Sect. 2.2.

Elliptical Galaxies. Several orbit studies connected with the onset of chaos in triaxial potentials, similar to real elliptical galaxies, have been undertaken (e.g. Udry & Pfenniger 1988; Martinet & Udry 1990; Schwarzschild 1993; Merritt & Fridman 1996). As for barred galaxies, chaos increases when triaxiality, central mass concentration, noise or asymmetries increase. Merritt & Valluri (1996) performed a detailed study on chaos and mixing in realistic potentials for ellipticals. They found that potentials with central density cusps present chaotic mixing timescales smaller than τ_H , especially near the center. As a result, triaxial galaxy centers should become axisymmetric with time. To my knowledge, the consequences on abundance profiles have not been studied so far; one could however expect a central flattening of abundance gradients, which is apparently not observed (Worthey, this volume).

2.2. Bars: Consequences for Stellar Abundance Profiles

N-body simulations represent a powerful tool to investigate non-linear phenomena, like those involving bar formation and evolution. Following previous studies of bar effects on abundance profiles (Friedli et al. 1994; Friedli & Benz 1995), I recently performed a new series of collisionless simulations of spontaneous bar formation (no element production); a particle-mesh method with $N = 400\,000$, a 3D exponential polar grid ($N_R = 61$, $N_\phi = 64$, $N_z = 243$), and a time-step $\Delta t = 0.1$ Myr are used. The central radial resolution is 20 pc, the vertical one 100 pc. Initial models are axisymmetric with pre-existing exponential abundance gradients, i.e.:

$$\frac{d \log(A/H)}{dX} \equiv A_X^{\text{reg}} = \text{constant} \quad [\text{dex kpc}^{-1}], \quad (1)$$

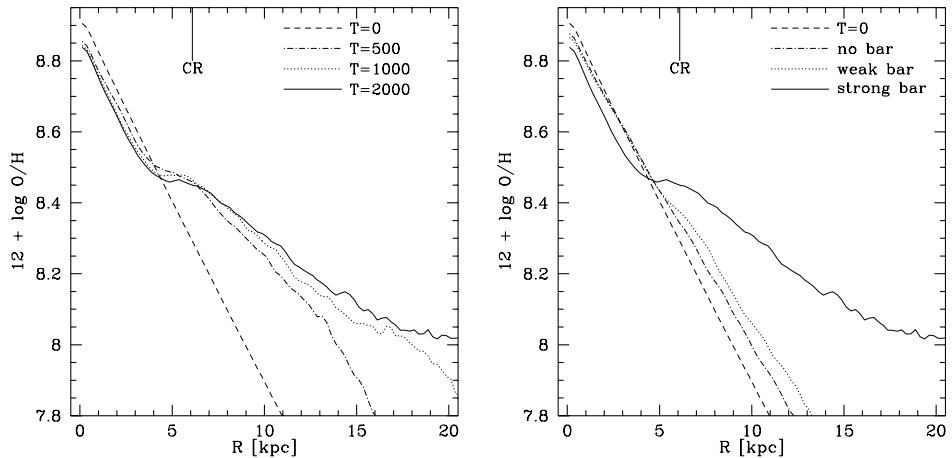


Figure 1. *Left.* Time evolution of the stellar radial abundance profile in a galaxy model forming a strong bar. CR indicates the corotation radius at $T=2000$ Myr. *Right.* Comparison of radial gradients between systems having no bar, a weak bar, or a strong one ($T=2000$ Myr).

where A stands for the chemical species studied (e.g. O for oxygen), X for radial R , azimuthal ϕ , or vertical z axes, and “reg” for the region considered.

Azimuthal Profile. The first case studied is $O_{\phi}^{\text{gal}} = -0.5$, and $O_R^{\text{gal}} = O_z^{\text{gal}} = 0.0$. Here, phase mixing is the dominant process. A very quick homogenization of the azimuthal gradient is observed both in axisymmetric and barred models, mixing being however ~ 1.5 faster in barred models. Like dynamical timescales, mixing timescales increase with R . After ~ 1 Gyr, no variations of mean abundances are detected in the whole disk.

Radial Profile. The “standard” case has $O_R^{\text{gal}} = -0.1$, and $O_{\phi}^{\text{gal}} = O_z^{\text{gal}} = 0.0$. Figure 1 (left) shows the time evolution of the radial abundance gradient in a model forming a strong bar (maximum bar axis ratio $(b/a)_{\text{max}} \approx 0.36$). The shape of this gradient evolves very quickly. Roughly speaking, it presents a break near CR; in more details, three major features can be highlighted: i) in the *disk region*, the gradient becomes much *flatter*, typically by a factor of 2–3, and the mean metallicity is strongly increased (only due to the redistribution of elements); ii) in the *bar region*, the gradient remains approximately the same, but the mean metallicity is decreased; iii) in the *corotation region*, a distinct *plateau* appears. Note that high spatial and temporal resolutions are required to be able to observe such a plateau. Recent observations of three barred galaxies by Beauchamp (1997) seem to indicate that the Mg_2 index presents such characteristics. However, it remains to be demonstrated that these features will be preserved after the conversion of the index into actual Mg abundances. Note that the projected isoabundances appear barred as well (Fig. 3, right).

To check that the bar is really the main engine which shapes the radial abundance gradient, additional systems with a weak bar (bar strength three times smaller than in the strong bar case) and no bar have also been computed.

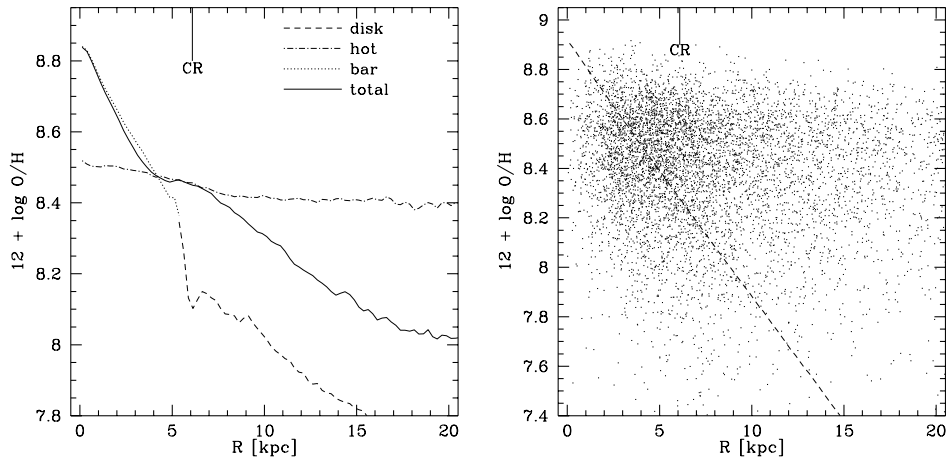


Figure 2. *Left.* Stellar radial abundance profiles in the strongly barred model for the total, bar, hot, and disk population of particles ($T=2000$ Myr). CR indicates the corotation radius. *Right.* Abundance scatter in the hot population. The dashed line is the initial value. Only 1/20 of the particles are plotted.

Figure 1 (right) compares the gradient of these various models at $T=2000$ Myr. Observed changes clearly appear to be dependent on the bar strength, as is also expected for chaotic mixing (see Sect. 2.1). The preponderant role of chaos is seen in Fig. 2 (left), where the respective gradients for the total, bar, hot, and disk populations have been plotted. The hot particles present a nearly flat gradient across the whole galaxy. Since they dominate the density distribution near CR, the origin of the plateau is disclosed! Although the mean gradient is flat, a huge abundance scatter, of the order of 1 dex, is present (Fig. 2, right).

The Sun is over-abundant with respect to the surrounding stars (e.g. Meyer et al. 1998). One explanation is that it was formed in a richer environment a few kpc closer to the galactic center, and then moved outwards. Since the Milky Way has a bar, a bar-induced diffusion might have caused this migration.

Vertical Profile. Finally, let us concentrate on the evolution of vertical abundance profiles by studying the case $O_z^{\text{gal}} = -0.5$, $O_R^{\text{gal}} = -0.1$, and $O_\phi^{\text{gal}} = 0.0$. Figure 3 (left) shows that the pre-existing steep vertical gradient is quickly flattened both in the bar and disk regions. A significant gradient only remains at $R=0$. In fact, projected isoabundances have a distinct boxy shape inside the bar (Fig. 3, right), more precisely inside the vertical Inner Lindblad Resonance (ILR). Bars and their associated vertical resonances have been recognized as very efficient engines to produce box/peanut shaped isodensity contours (Pfenniger 1985; Combes et al. 1990; Pfenniger & Friedli 1991). And this morphology is even more pronounced when the abundances are plotted. In models having $O_z^{\text{gal}}=0$ at the beginning, a moderate negative vertical gradient appears at $R=0$, and a *positive* vertical gradient is observed in the disk. It results from the z - and R -diffusion of the hot metal-rich particles. The box/peanut shape is also becoming more extreme to be definitely X-shaped in this case.

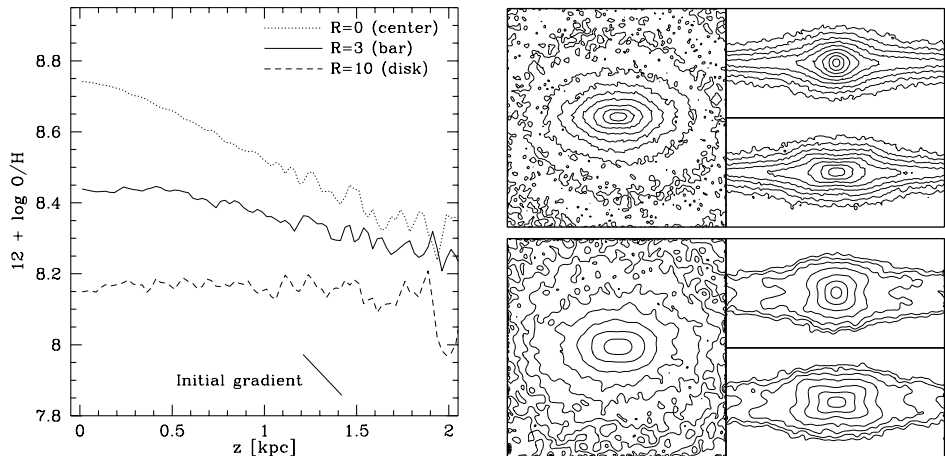


Figure 3. *Left.* Stellar vertical abundance gradients at various radii R in a galaxy model forming a strong bar ($T = 1000$ Myr). *Right.* Projected isodensity (top) and isoabundance (bottom) stellar contours in the three principal planes ($T = 2000$ Myr). The scales are logarithmic and the frames are 8 kpc wide. Note the striking boxy morphology.

3. Mixing and Transfer of Gas

3.1. Bar-Induced Gas Flows and Star Formation

If gas moves on intersecting trajectories (e.g. chaotic orbits or periodic orbits with loops), it will be shocked. Kinetic energy is first transformed into thermal energy, which in turn is radiated away out of the galaxy by escaping photons, since radiative cooling is generally very efficient. In barred galaxies, significant energy dissipation via shocks, as well as angular momentum transport via gravitational torques, result in intricate transfers (flows) and mixing of cold or warm gas. This has been demonstrated by hydrodynamical simulations (Prendergast 1983; Athanassoula 1992; Friedli & Benz 1993; Friedli et al. 1994; Piner et al. 1995). Very roughly, one observes: i) net gas inflows inside CR towards the center, channeled along the bar major axis; ii) outflows outside CR towards the Outer Lindblad Resonance via bi-symmetric spiral arms. Inflow/outflow rates are proportional to the bar strength, but they also depend on other parameters like the gas mass fraction. While the effects of “simple” radial gas flows can be incorporated in galactic chemical evolution models (e.g. Edmunds & Greenhow 1995), such an approach appears untractable for realistic flows in strongly triaxial systems, where self-consistent numerical simulations are necessary.

Strictly speaking, star formation (SF), and consequently element production, are beyond the scope of this review! However, when dealing with gaseous abundances, it is natural to introduce SF in the models, which entails important results (Sect. 3.2). The possible connections between bars and SF have been widely studied (Hawarden et al. 1986; Kennicutt 1994; Contini 1996; Martinet & Friedli 1997; Martin & Friedli 1997; and references therein). One of the main results is that young ($\lesssim 1$ Gyr) and strong bars significantly enhance SF. Also, the sites of massive star formation within strong bars evolve, over a few

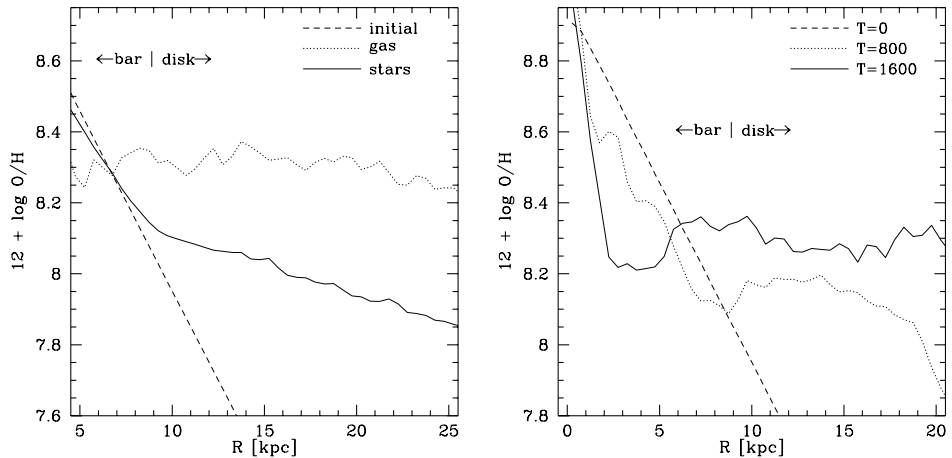


Figure 4. *Left.* Comparison between stellar and gaseous abundance profiles in a strongly barred model for the disk region ($T = 2000$ Myr). *Right.* Time evolution of the gaseous abundance gradient. Note the distinct breaks near the end of the bar and in the disk at $T = 800$ Myr.

Gyr, from an extended chain-like distribution along the bar major axis and the center, to a concentrated nuclear ring-like morphology once ILRs appear.

3.2. Bars: Consequences for Gaseous Abundances Profiles

The previous section clearly tells us that bars should deeply influence the chemical evolution of galaxies. In particular, one expects a quick radial homogenization of the cold or warm gas, which leads to a *flattening* of any abundance gradient. This intuition is nicely confirmed both by observations (Pagel & Edmunds 1981; Vila-Costas & Edmunds 1992; Martin & Roy 1994; Roy 1996) and numerical simulations (Friedli et al. 1994; Friedli & Benz 1995; Martinet & Friedli 1997). The most recent studies also found that the degree of flattening is directly proportional to the bar strength (see Martin, this volume). After 1–2 Gyr, the gaseous abundance gradient clearly becomes flatter than the stellar one in the disk region (Fig. 4, left), and the gas phase is typically over-abundant by $\sim 0.2 - 0.4$ dex with respect to the averaged stellar abundance.

Another recent discovery, mainly due to the boost of measurable H II regions per galaxy, concerns the presence of *breaks* in the radial abundance profiles (Zaritsky et al. 1994; Martin & Roy 1995; Roy & Walsh 1997), i.e. the gradient appears relatively steep in the bar region, whereas it is very shallow in the disk region (“steep-shallow break”). Numerical models indicate that such a feature is typical in young and strong bars (Martinet & Friedli 1997). The vigorous star formation along the bar major axis is indeed able to produce enough new elements to compensate the dilution resulting from the bar-driven gas inflow. A clear break occurs near the CR and lasts for about half a Gyr (Fig. 4, right). At this stage, at a given radius, spiral arms are also enriched by a few dex with respect to interarm regions. These abundance fluctuations are then progressively erased by azimuthal mixing processes. It is interesting to note that the abundance scatter in the disk of NGC 3359 is approximately

0.4 dex, i.e. twice the usual observed value. This galaxy is precisely thought to have a very young bar (Martin & Roy 1995).

Another break could be observed in the outer part of the disk when the gradient steepens again (“shallow-steep break”). There, the long mixing timescale somewhat delays the complete flattening of the abundance gradient. Owing to observational difficulties, this predicted second break has not yet been detected.

The central starburst generated by the bar formation may also produce a *metal-rich core* (Friedli et al. 1994). The determination of the very central abundances is very difficult and uncertain. Circumnuclear ones are however more reliable; they are generally relatively high, but very similar in barred and unbarred galaxies (Storchi-Bergmann et al. 1996). This apparent non-enrichment of the nucleus of barred galaxies might be an indication of metal outflows in superwinds (e.g. Heckman 1997). These metals could thus either be locked in the hot gaseous phase, or have been ejected from the galaxy. They might also have been swallowed by a central supermassive black hole, if present.

4. Summary

In strongly barred galaxies, dynamically-induced abundance profiles are functions of both time and space, and major characteristics can schematically be summarized, using the definitions of Eq. 1, as follows:

$$\begin{array}{llll}
 \textit{Stars:} & |A_R^{\text{bar}}| > |A_R^{\text{disk}}|, & A_R^{\text{CR}} \approx 0 & A_\phi^{\text{gal}} \approx 0 & A_z^{\text{box}} \approx 0 \\
 \textit{Gas:} & |A_R^{\text{bar}}| > |A_R^{\text{disk}}| & & A_\phi^{\text{gal}} \neq 0 & \text{(Young bar)} \\
 & & A_R^{\text{gal}} \approx 0 & A_\phi^{\text{gal}} \approx 0 & \text{(Old bar)}
 \end{array}$$

5. Conclusion

Barred dynamics significantly alters stellar and gaseous abundance profiles in only a fraction of a Hubble time. Strong bars have both a *direct* influence via very efficient mixing and transfer of metals, and an *indirect* effect via important element production through the possible enhancement of star formation.

In order to properly and fully interpret the observed abundance profiles in galaxies, galactic chemical evolution models should clearly take into account *dynamics*, particularly the triaxial one, in addition to the classical and basic ingredients like yields, IMF, and star formation rate.

Acknowledgments. I thank L. Drissen and J.-R. Roy for a careful reading of the manuscript and useful comments. I am indebted to P. Martin for having initiated me into the topic of abundance profiles a few years ago! I acknowledge the Swiss National Science Foundation (FNRS) for its support through an “Advanced Researcher” fellowship, and the Université Laval for its kind hospitality.

References

- Athanassoula, E. 1992, MNRAS, 259, 345
 Athanassoula, E., Bienaymé, O., Martinet, L., & Pfenniger, D. 1983, A&A, 127, 349

- Beauchamp, D. 1997, Ph.D. thesis, Université Laval, Québec, Canada
- Binney, J., & Lacey, C. 1988, MNRAS, 230, 597
- Binney, J., & Tremaine, S. 1987, in Galactic Dynamics. (Princeton: Princeton University Press), 269
- Combes, F., Debbasch, F., Friedli, D., & Pfenniger, D. 1990, A&A, 233, 82
- Contini, T. 1996, Ph.D. thesis, Université Paul Sabatier, Toulouse, France
- Contopoulos, G., & Grosbøl, P. 1989, A&AR, 1, 261
- Edmunds, M.G., & Greenhow, R.M. 1995, MNRAS, 272, 241
- Friedli, D., & Benz, W. 1993, A&A, 268, 65
- Friedli, D., & Benz, W. 1995, A&A, 301, 64
- Friedli, D., Benz, W., & Kennicutt, R. 1994, ApJ, 430, L10
- Habid, S., Kandrup, H.E., & Mahon, M.E. 1997, ApJ, 480, 155
- Hasan, H., & Norman, C.A. 1990, ApJ, 361, 69
- Hawarden, T.G., Mountain C.M., Leggett S.K., & Puxley P.J. 1986, MNRAS, 221, 41p
- Heckman, T. 1997, RevMexAA (serie de conferencias), 6, 156
- Kennicutt, R.C. 1994, in Mass-Transfer Induced Activity in Galaxies, ed. I. Shlosman. (Cambridge: Cambridge University Press), 131
- Martin, P., & Roy, J.-R. 1994, ApJ, 424, 599
- Martin, P., & Roy, J.-R. 1995, ApJ, 445, 16
- Martin, P., & Friedli, D. 1997, A&A, 326, 449
- Martinet, L., & Udry, S. 1990, A&A, 235, 69
- Martinet, L., & Friedli, D. 1997, A&A, 323, 363
- Merritt, D., & Fridman, T. 1996, ApJ, 460, 136
- Merritt, D., & Valluri, M. 1996, ApJ, 471, 82
- Meyer, D.M., Jura, M., & Cardelli, J.A. 1998, ApJ, 493, 222
- Monteverde, M.I., Herrero, A., Lennon, D.J., & Kudritzki, R.-P. 1997, ApJ, 474, L107
- Odehahn, S.C. 1996, in Barred Galaxies, IAU Coll. 157, eds. R. Buta et al. ASP Vol.91 (San Francisco: ASP), 30
- Ollé, M., & Pfenniger, D. 1998, A&A, in press
- Pagel, B.E.J., & Edmunds, M.G. 1981, ARA&A, 19, 77
- Pfenniger, D. 1985, A&A, 150, 112
- Pfenniger, D., & Friedli, D. 1991, A&A, 252, 75
- Piner, B.G., Stone, J.M., & Teuben, P.J. 1995, ApJ, 449, 508
- Prendergast, K.H. 1983, in Internal Kinematics and Dynamics of Galaxies, ed. E. Athanassoula. (Dordrecht: Reidel), 215
- Roy, J.-R. 1996, in Barred Galaxies, eds. R. Buta et al. IAU Coll. 157, ASP Vol.91 (San Francisco: ASP), 63
- Roy, J.-R., & Kunth, D. 1995, A&A, 294, 432
- Roy, J.-R., & Walsh, J.R. 1997, MNRAS, 288, 715
- Schwarzschild, M. 1993, ApJ, 409, 563
- Sellwood, J., & Wilkinson, A. 1993, Rep. Prog. Phys., 56, 173
- Sparke, L., & Sellwood, J.A. 1987, MNRAS, 225, 653
- Storchi-Bergmann, T., Wilson, A.S., & Baldwin, J.A. 1996, ApJ, 460, 252
- Udry, S., & Pfenniger, D. 1988, A&A, 198, 135
- Vila-Costa, M.B., & Edmunds, M.G. 1992, MNRAS, 259, 121
- Zaritsky, D., Kennicutt, R.C., & Huchra, J.P. 1994, ApJ, 420, 8